AIAA SciTech Forum
6-10 January 2020, Orlando, FL
AIAA Scitech 2020 Forum

10.2514/6.2020-0162

Aero-structural Design Tool for Advanced Exhaust Systems

Nikhil Nigam[1], Sricharan Ayyalasomayajula[2], Yuye Tang[3], and Padmanabha Ketha[4]
Intelligent Automation Inc., Rockville, MD, 20855

Victorien Menier[5] and Juan J. Alonso[6]
Stanford University, Stanford, CA, 94305

Rick W. Fenrich[7]
Arevo Inc., Milipitas, CA, 95035

Increasing fuel demand and acoustic considerations have resulted in a need for advanced non-axisymmetric and variable geometry nozzles. The complexity of the flow can however, result in pre-mature structural failure in certain cases. In order to make the nozzles more efficient, quiet, and structurally safe, there is a need to revisit the design of such exhaust systems. The flow of exhaust gases through the exit nozzle plays a critical part in the performance of an engine and its acoustic signature. In order to accurately capture the flow physics, the design of advanced nozzle configurations requires high-fidelity aerodynamic analysis. At the same time, structural analysis is necessary to avoid heavy or structurally unsafe designs, and to ensure that the resulting structure can withstand the thermal and mechanical loads that are imposed on the nozzle. Hence, there is a need to conduct high-fidelity coupled aero-structural analyses within a design optimization framework. To this end, we have been developing the COMANDO (COupled Multiphysics ANalysis and Design Optimization) framework for the design of advanced exhaust systems. In this paper, we describe our efforts to enable a multi-fidelity computational fluid dynamics analysis capability, based largely on Euler and Reynolds-Averaged Navier-Stokes (RANS) simulations using the SU2 solver. For structural analysis, ANSYS Finite Element Analysis (FEA) has been coupled with the RANS-based analysis. Moreover, since the substructure design is crucial for managing thermoelastic loads, a nested optimization capability has been developed. In order to facilitate the use of the tool and portability, we also describe our initial efforts in interface development and dockerization. These methods are demonstrated for an axisymmetric modified NPARC nozzle.

I. Introduction

A. Background

The fuel costs for the DOD were about $17 billion in 2011 [1], while the U.S. Navy (USN) alone uses about 1.3 billion gallons of fuel per year [2]; and in 2003, 73% of DOD's petroleum use was accounted for by aircraft [1] [3]. NASA also has similar fuel concerns [4] in addition to issues with local and global emissions and noise [5]. Noise is also an important issue for the USN because of the harsh acoustic environment created during operations of these aircraft on aircraft carriers and the impact to communities around naval air bases and training sites [6]. The extreme levels of acoustic radiation emitted from jets mandate the need to reduce jet noise at its source, through modifications to nozzle geometry, for example [7]. To address these concerns, the propulsion systems community has been investigating several innovative nozzle concepts (such as ejector, mixer-ejector, plug, SERN, altitude compensating, lobed and chevron nozzles [8] [6] [9]). However, there is a need to understand the flow and structure physics to design such concepts effectively.

1 Lead Scientist, Signals Analysis and Controls, AIAA Member.
2 Sr. Research Scientist, Distributed Intelligent Systems, AIAA Member.
3 Sr. Research Scientist, Signals Analysis and Controls.
4 Lead Software Developer, Signals Analysis and Controls.
5 Post-doctoral Appointment, Department of Aeronautics and Astronautics, AIAA Student Member.
6 Professor, Department of Aeronautics and Astronautics, AIAA Associate Fellow.
7 Member of Technical Staff, AIAA Member.

Jet and nozzle flows generally include complex turbulent mixing, as well as temperature and compressibility effects which may be further complicated by chemical reactions and shear layer instabilities. Reynolds-Averaged Navier-Stokes (RANS) methods require turbulence models for mathematical closure, thereby introducing an empirical correction into the equations [11]. In general, they have been deemed insufficient for capturing unsteady flow features, although RANS remains a key tool for aerodynamic design. Combining Large Eddy Simulation (LES) with RANS, *e.g.* via multi-fidelity modeling, may help us achieve the required fidelity without unduly sacrificing speed for design.

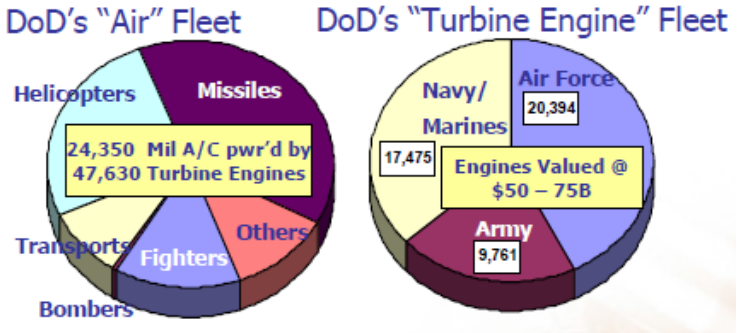

Figure 1: DOD's aircraft and turbine engine investment [10].

In general, there exists a lack of research on coupled aero-structural nozzle design, which entails its own suite of problems [12]. The structural analysis required for accurate stress/deformation computation helps determine key nozzle design parameters such as the length and thickness distribution. Structural design also determines the weight of the nozzle and, in some unsteady flows, aero-structural phenomena may become important [12]. The design of thermal structures in particular brings additional considerations [13]. For instance, increasing thicknesses of structural members may actually be detrimental from thermal stress point of view [14]. Some limited work on design of nozzles has been performed at NASA [15] using Multidisciplinary Design Optimization (MDO), but it has been limited to relatively lower-fidelity aerodynamic and structural analyses [16]. The substructure design is also highly dependent on the particular nozzle and flow conditions – so it may need to be redesigned for each new configuration studied. Traditional design has used sequential techniques, focusing on aerodynamic design first; followed by structural design. However, this leads to design inflexibility and very heavy structures in certain cases. Modern design and analysis methods will allow revisiting the nozzle design, engine-airframe integration, and similar issues.

B. Our Contributions

To effectively address these nozzle design issues, our team has been developing COMANDO, a multi-fidelity, multi-physics based analysis and design optimization framework for advanced exhaust systems. Figure 2 shows the envisioned composition of COMANDO. The key analyses in the nozzle design involve aerodynamics and structures (and capturing the coupling between them). We have developed Euler- and RANS-based capabilities for nozzle analysis, using the SU2 solver [17]. In addition, we have setup a Wall Modeled LES (WMLES)-based analysis capability using the CharlesX solver. Currently a similar capability is also being developed by our team in SU2, in the form of a higher order Discontinuous Galerkin (DG) solver. These tools can be integrated into COMANDO through a variable-fidelity analysis technique based on response surfaces [18] [19]. However, the focus of this paper is the use of Euler/RANS for design optimization with the eventual goal of using LES information for design in the future.

In parallel, we have developed a Finite Element Analysis (FEA)-based structural analysis to determine the weight of the nozzle and stresses/deflections, which become important design criteria. We have also developed an FEA-based structural optimization architecture to determine optimal nozzle/substructure thicknesses. Such techniques are being investigated in the aircraft design community to obtain higher-fidelity weight estimates during the conceptual design phase [20] [21]. Once the FEA and Computational Fluid Dynamics (CFD) analyses are setup, we also need to share loads (both mechanical and thermal) and displacements between them. While, ideally, a tightly coupled nonlinear structural analysis may be eventually desirable; certain research has shown the feasibility of using quasi-steady linear analysis for such applications [22]. Hence, as a starting point, we have used linear structural analysis coupled loosely to aerodynamics. This task is far from trivial due to the differences in meshes between the two disciplines [12]. We have developed two methods for the transfer of information between fluid and structures. One is a simple interpolation technique that we use for the axisymmetric nozzle. Another is a rigorous consistent and conservative load transfer technique to transfer loads/displacements between CFD and FEA. For the purposes of this paper, we will be focusing on the former.

The aerodynamic (Euler and RANS) analysis, structural analysis, and aero-structural coupling have been integrated into an MDO architecture that leverages the DAKOTA framework [23]. Both direct, and surrogate-based optimizations have been developed, which have been demonstrated for a modified NPARC Alliance nozzle [24]. Substructure optimization has also been implemented within the structural analysis. Finally, in order to make these capabilities easily accessible to the end user, we have been integrating the technologies into a toolset with a suitable interface. Docker technology has been used to enable easy portability of the tool as well. This paper continues the work in Ref. [25], and describes our efforts in setting up the aero-structural analyses, optimizations and interfaces. Some of the initial effort in setting up the framework was described in a previous paper by our team [25] – this paper describes the additional work performed, with some overlap for completeness.

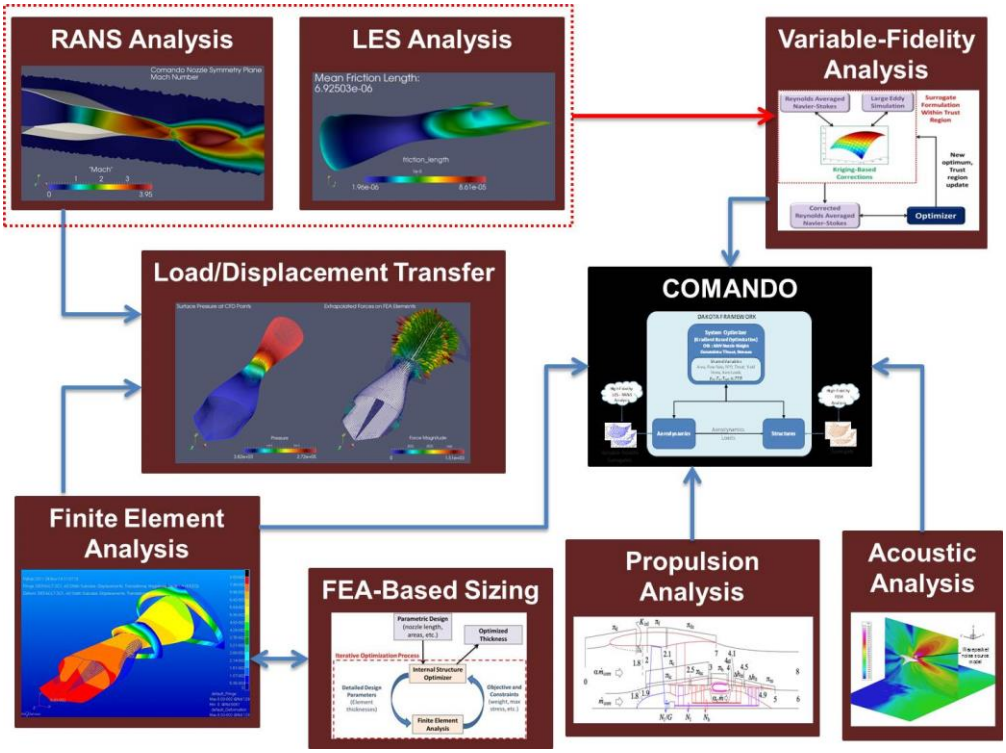

Figure 2: Basic architecture and components of the envisioned COMANDO tool.

II. Nozzle Concept for Studies

We have been investigating several nozzle concepts covering different aspects. An Unmanned Combat Air Vehicle (UCAV)-like nozzle was previously studied to demonstrate the analysis setup [26]. We have also been investigating the Wellborn S-Duct [27] for validation of a Wall Modeled Large Eddy Simulation (WMLES) capability that is being developed in parallel. However, for the core development of the design optimization architecture we focus on a simple axisymmetric nozzle as the test case since it enables a rapid simulation capability. This particular nozzle is available in the NPARC Alliance website [24], and has been extensively studied in the past. The nozzle operates at approximately 2.2 Mach, and the detailed geometry is available from the NPARC website. This nozzle characterizes the phenomenon of axisymmetric mixing in turbulent compressible fluids. In order to keep the flow characteristics simple, the nozzle operates in quiescent air.

This nozzle has been modified by our team, in prior work, to match the airflow and thrust of a P&W F-100 jet engine (geometry, mesh and Mach contours are shown in Figure 3). The axisymmetric geometry also allows us to easily represent the inner duct using a spline (which can rotated about the longitudinal axis to generate the entire solid). In the design optimization, a subset of the control points of the spline are considered as design variables, thereby enabling efficient geometry control. More details on the configuration can be found in our prior work [25].

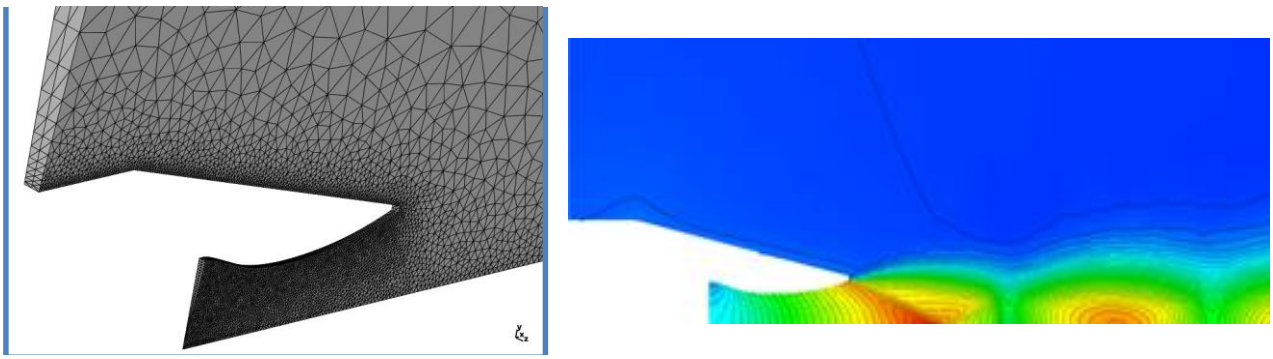

Figure 3: Modified NPARC nozzle mesh and Mach contours.

III. Aerodynamic Analysis

The highest fidelity of interest is WMLES capability. However, the technology is still pre-mature for direct incorporation of LES in design architectures. One possibility for approximating the accuracy of LES for design purposes is to combine RANS and LES-based information using surrogate modeling. However, in this paper we focus on a multi-fidelity aerodynamic analysis framework comprised of three fidelities: (1) a quasi-1D analysis based on gas dynamic equations, (2) an Euler solver, and (3) a RANS solver.

In the quasi-1D analysis the area-averaged 1D Navier-Stokes equations are solved along the length of the nozzle. The aerodynamic analysis is additionally coupled with a simplified heat transfer model which models heat transfer via conduction and convection with thermal resistances aligned in the radial direction.

The Euler and RANS aerodynamic models provide an increased level of fidelity. The well-established open source finite volume CFD solver SU2 is used for the solution of the Euler and RANS equations [17]. A standard edge-based data structure is used in SU2 and the control volumes are constructed using a median-dual, vertex-based scheme. The convective fluxes are discretized using the second-order accurate JST scheme [28] and the Menter SST turbulence model [11] is employed for viscous simulations. Time integration is performed using an Euler implicit method and the linear system is solved using the Generalized Minimum Residual (GMRES) method. In order to damp low-frequency errors an agglomeration multigrid method is employed. Since even small changes in the nozzle shape can have a dramatic impact on the flow physics, particularly near the throat of the nozzle, flow parameters must be carefully tuned. Figure 3 shows a representative solution for the Euler model.

For each the Euler and RANS models a set of increasingly refined baseline meshes was crafted ranging from coarse to fine (see Figure 3). An initial mesh was generated using Gmsh [29] with different levels of refinement for the nozzle interior, exit, plume, mid-field, and far-field regions. Then the mesh was remeshed using the Feflo.a-AMG Inria library to satisfy mesh size requirements [30]. For RANS meshes a quasi-structured boundary layer mesh is also generated using Bloom, a viscous mesh generator developed at Inria [31]. During optimization, these baseline meshes are deformed to fit the nozzle geometry by analytically projecting the baseline mesh onto the new geometry and then running the SU2 mesh deformation module to ensure good quality of the volume mesh.

Overall, the aerodynamic models present a range of fidelities that allow for rapid estimation of aerodynamic performance on a wide variety of designs, as well as detailed study of interesting configurations. Several robustness studies were performed in the nozzle design space to ensure the solvers converged reasonably well, as presented in Ref. [32].

IV. Structural Analysis

A key requirement driving this research is the need to capture the structural response of the system to get a better understanding of nozzle weight and stiffness for candidate designs. The structural design and analysis is complicated by two factors:

1) In order to understand the structural response, the nozzle duct cannot be studied in isolation. Modeling the connection of the nozzle with the airframe / outer duct is crucial. Thus, the substructure connecting the nozzle to the outer duct must be modeled.
2) The thermal loads are the driving factor in most nozzle designs, which necessitates a thermoelastic analysis of the structure. Moreover, the design choices for thermoelastic structures can often be counter-intuitive, resulting in structures that are difficult to design.

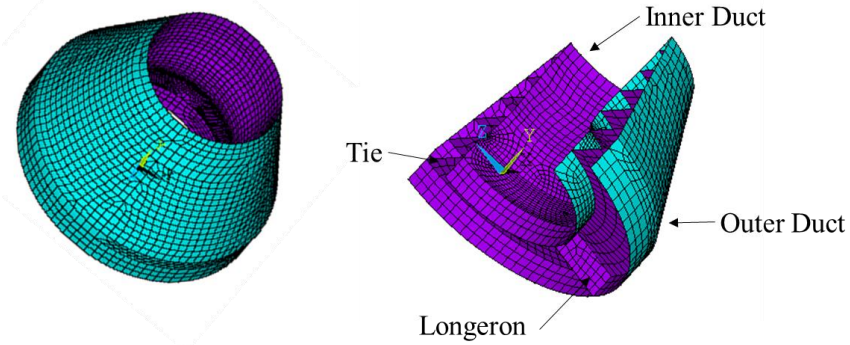

Figure 4: 3D Nozzle FEM and illustration of substructure members.

Due to the challenging operating environment of thermally loaded structures, and multiple failure criteria (including strength, low cycle fatigue, high cycle fatigue, creep, etc.), the design of these structural members in not straightforward. Topology optimization can help design such complex structures, but at an exorbitant computational expense. For COMANDO, the aim is to develop a capability to design nozzles with different structural and aerodynamic requirements. Thus the capability should not be tied to a specific substructure/nozzle concept – instead, we require a capability that allows us to capture the relevant physics of the process without being too specific and expensive to evaluate. Hence, we did not attempt to use topology optimization in the process, and only the relevant level of details of the substructure were included in the analysis. A

schematic of the model for the exhaust duct structure is shown in Figure 4. The substructure members consist of ties (circumferential members connecting inner and outer duct at several axial stations) and longerons (axial stiffners along the length of the nozzle). The thickness of the inner duct and outer duct are 0.005 m and 0.010 m, respectively (baseline values). There are a total of six ties connecting the inner duct to the outer duct, and the thickness is chosen to be 0.010 m uniformly. Four longerons symmetrically placed (90° angular separation) with a uniform thickness of 0.010 m are also shown. Moreover, we studied a dual liner concept for the inner duct as well. Such designs are often used to avoid loading a single duct with both mechanical and thermal loads, as shown in **Figure 5**. The inner liner bears mostly thermal loads; the outer liner is subjected to most of the pressure loads. It is assumed that there is a 0.015m air gap in between, which is modeled as a conductive medium with a thermal conductivity of 0.06 W/mK.

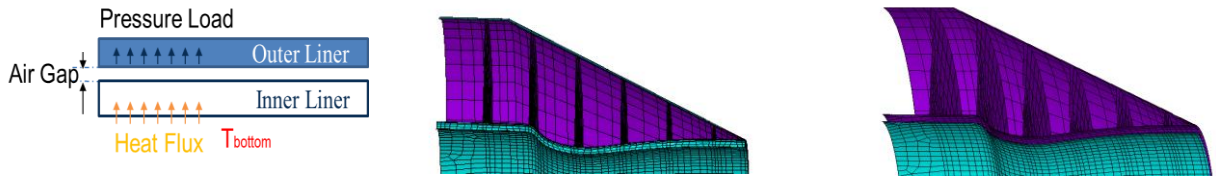

(a) Dual liner concept (b) FE model for thermal analysis (c) FE model for mechanical analysis

Figure 5: Inner duct dual liner design and FEM details.

Details of the structural modeling and results from the analysis, were presented in prior work by our team [25]. Based on those studies, certain improvements were made to the choice of substructure member locations, materials, etc. in this work. Some of the key changes are described below.

1) In previous work, we used Inconel 625 for the inner liner, and Titanium 6245 for the rest of the structure. However, in this work, we have used Titanium 6245 for the entire structure.
2) Prior work involved modeling the air cavities (formed between substructure members) as conductive media for simplicity. In this work, we also studied a simplified convection model (described below) for the same and compared to the former model.
3) Buckling analysis was incorporated in the analysis, to provide an additional constraint in the design, *i.e.* to avoid very thin substructure members in the optimization.

A. Convective Model

The simplified convective process models convection as a one-dimensional flow process between the inner and outer ducts (assuming there is no convection between the ties). For each closed cavity, convective boundary conditions were applied both on the outer liner outer surfaces and the outer duct inner surfaces. Convection is related to heat flux by use of Newton's law of cooling:

$$q/A = h(t_s - t_f),$$

where q/A is heat flux out of the face, h is the film coefficient, t_s is the temperature on the face, and t_f is the bulk fluid temperature.

t_f is assumed to be a uniform value in each cavity, which can be found by forcing the total energy flow out the outer liner equal to the energy flow into the outer duct

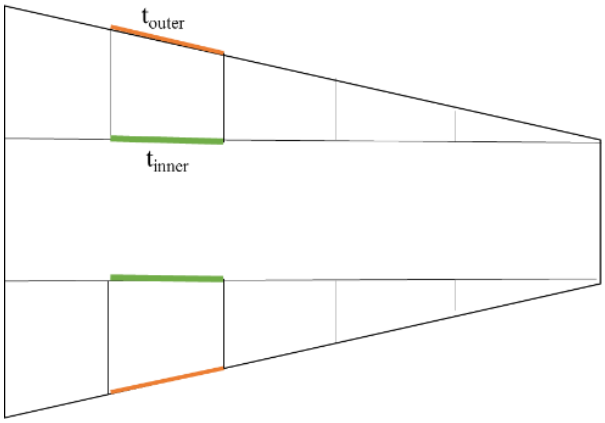

Figure 6: Illustration of the convective modeling approach.

$$\sum q = \sum A_i h(t_i - t_f) = 0,$$
$$t_f = \sum A_i t_i / \sum A_i ,$$

where t_i represents the surfaces in the cavity. During thermal analysis, the average temperature t_f is computed and the convection boundary conditions are reassigned until t_f converges to a constant value.

In order to understand the effects of structural design choices, we conducted several studies that guided our decisions in setting up COMANDO. A summary of the different models constructed for this purpose is shown in **Table** 1.

Table 1: Different FE models studied.

Modeling Techniques	**Model Description**			
	Single Liner Model with Ties	Single Liner Model with Ties and Longerons	Dual Liner Model with Conductive Air	Dual Liner Model with Convective Air
Heat Conduction in Metal Structure	✓	✓	✓	✓
Heat Conduction in Air Gap between Liners	N/A	N/A	✓	✓
Heat Conduction in Closed Cavities	✗	✗	✓	✗
Heat Convection in Closed Cavities	✗	✗	✗	✓
Thermal FE Mesh	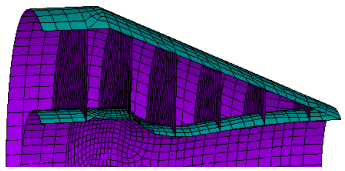			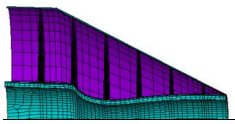
Structural FE Mesh			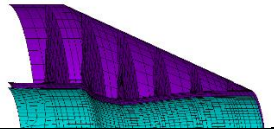	

Several results for single and dual liner cases were presented in our prior work, and are not presented here for brevity. We compared the convective and conductive air models for the air cavities as well. Since the results were similar, we decided to continue with the simpler conductive medium model for air in subsequent work.

B. Buckling Analysis

Buckling of structures, though not a major concern in several applications, can become a critical design constraint for the design of thin-walled structures, especially thermally loaded substructure members. Hence, we incorporated a capability for performing buckling analysis as well for the structure. This capability was developed in ANSYS, which can solve the geometric instability problem at a variety of fidelities ranging from linear (eigenvalue buckling) to nonlinear, and post-buckling analysis. Although less precise than nonlinear buckling analysis, eigenvalue buckling analysis is an easy approximate method to determine the critical loads for buckling and buckling modes. It is important to remember that the need for this analysis is to guide the design in the appropriate direction and not let the substructure optimization push the thicknesses to a minimum. So, extremely accurate buckling analysis is not required. The computational time for the eigenvalue buckling is also usually significantly faster than a nonlinear buckling analysis.

The analysis is composed of two steps. First, a static structural analysis is performed considering the loads and boundary conditions. In our case, the thermal-mechanical sequential analysis is carried out, and the loads, boundary conditions, and stress state of the nozzle can be obtained. Second, linear buckling analysis is performed. In this way, the effects of pre-stress from the static analysis can be considered. In the post analysis, the buckling mode shapes and load multipliers can be reviewed. The

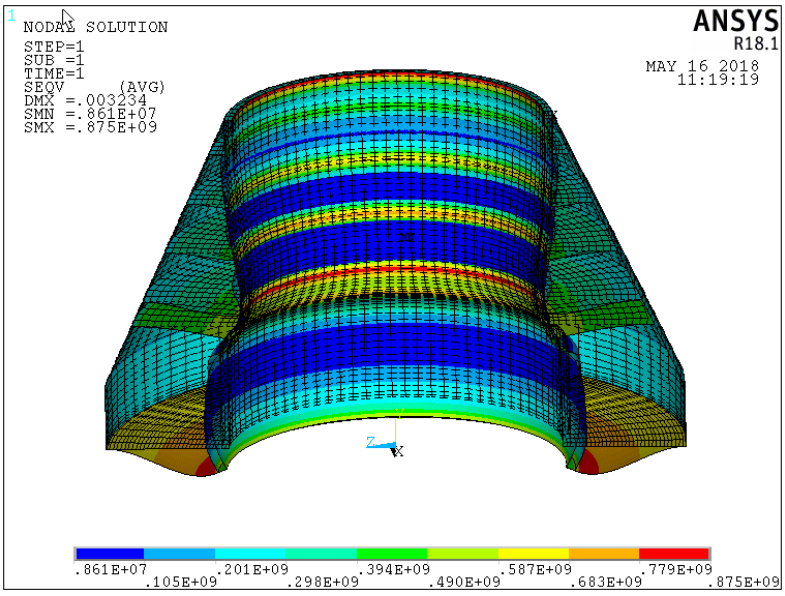

Figure 7: Stress distribution in the static solution used for buckling analysis.

critical buckling load can be determined by the loading inputs times the load multiplier. Linear analysis was implemented in ANSYS APDL by adding a short script
after the thermoelastic analysis. The first buckling load factor is output, which can be used in a constraint during optimization.

A feasible solution (in terms of the thermoelastic static analysis) was selected as the initial point for the buckling analysis (the corresponding stress distribution is shown in Figure 7). Examples of the buckling modes are shown in Figure 8. As expected, buckling will first be observed in the 6th and 5th ties, which are larger aspect ratio than others. We also tried cases for pure mechanical and pure thermal loads and based on the resulting load multiplier for buckling, we concluded that it is primarily the thermal loads that can lead to buckling for this nozzle and substructure geometry. Similar tests were performed to make sure that the buckling analysis was producing reasonable results, and then this analysis was incorporated in the substructure design optimization.

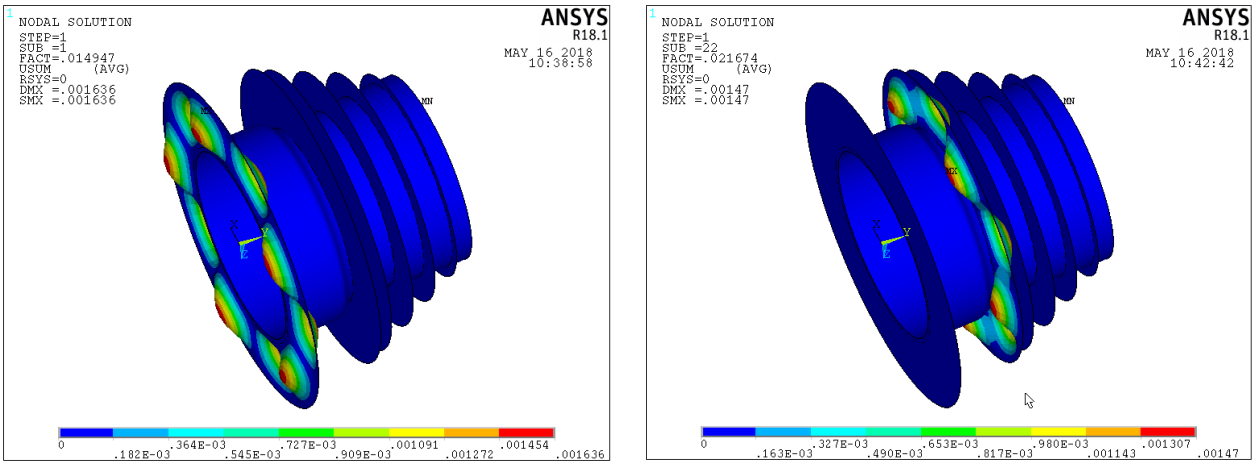

Figure 8: Examples of buckling modes (for buckling in 6th and 5th ties, respectively).

V. Aero-Structural Coupling

We have implemented two kinds of aero-structural couplings in previous work: (1) a simple interpolation capability for axisymmetric nozzles that basically transfers loads from 2D aerodynamic analysis to full 3D structural analysis using spline-based interpolation [25], and (2) a consistent and conservative fluid structure interface capability for more complex geometries [26]. The latter capability is being improved for application to other nozzles and inlets as well, in some ongoing work. But we used the former capability for saving computational expense, for the purposes of this research (which is using the axisymmetric modified NPARC nozzle as test case). Since details of the capability were presented in a prior publication [25], we will not repeat them here.

VI. Multidisciplinary Design Optimization

The eventual goal for COMANDO tool is a capability to design advanced exhaust systems at a conceptual/preliminary design level. This is an inherently multidisciplinary design problem as the role and interaction of aerodynamics and structures is critical. Towards this end, we have been developing a design optimization architecture that works with a small number of design variables and captures the relevant physics to guide the design. Below we present the details of the ongoing work on development of design capability.

A. Design Space Parameterization

The first step in the design process is to characterize the design space by selecting appropriate design variables and parameters. In this study, we have assumed that the inlet area and flow conditions are fixed (*i.e.*, we are not changing the engine design). In addition, flight conditions, material properties and number of ties/longerons are fixed. Hence, we vary the inner duct geometry and substructure member thicknesses. A simple way to parameterize the inner duct geometry is to use location of the throat, x_{throat}, length of the nozzle, L_{nozzle}, nozzle throat area, A_{throat}, and nozzle exit area, A_{exit}. In addition, we assume constant thickness for each substructure member and the nozzle. As a result, there is one design variable associated with each substructure member thickness.

The nozzle inner duct is represented using a B-spline. In order to keep the computational expense low and facilitate the mapping between the design variables above and the nozzle shape, we use a simplified 9-knot representation of the nozzle inner duct, as outlined in our prior work [25]. This representation does not afford the flexibility of a more detailed representation, but is adequate for our initial design activity.

C. MDO Architecture

To determine the appropriate MDO architecture, we first formulate a system level optimization problem and then investigate options for decomposing the problem. The system level optimization problem can be posed as:

$$
\begin{gathered}
Minimize W \\
w.r.t. L_{nozzle}, A_{throat}, A_{exit}, x_t, t_{nozzle}, t_{tie}, t_{longeron} \\
subject\ to: \\
Thrust \geq Thrust_{required} \\
max\big(T(x)\big) \leq T_{max} \\
max\big(\sigma(x,y,z)\big) \leq \sigma_{max}
\end{gathered}
$$

where W is the weight of the nozzle (including substructure), t is the thickness of the structural member, T is the temperature (a function of temperature), and σ is the stress. In other words, we want to minimize the weight, subject to constraints on aerodynamic performance (thrust/specific fuel consumption), temperature and stresses. Note that we are only constraining the maximum values of stress and temperature, instead of a large number of constraints associated with temperatures at each grid point. Although this can introduce nonlinearities or non-smooth behavior in the constraints, such behavior will be investigated during use. Note that the t_{tie} and $t_{longeron}$ can be a single variable associated with each member type, or a different variable for each member.

In deciding the particular MDO architecture, several options are available: monolithic vs. distributed [33], single vs. multiple optimizers [34], direct analysis vs. surrogate-based [19], and additional details of distributed architectures. The choice is intimately related with the exact problem to be solved and details of the parameterization. In our case, since the aerodynamic and structures are relatively tightly coupled, the monolithic optimization architecture emerges as a natural choice. In this architecture, all the analyses are coupled together (Multidisciplinary Analysis (MDA)) with a single optimizer driving the solution (refer Figure 9). This architecture is simple to implement and is perhaps the most robust (in terms of converging to the solution), but also the most expensive. To somewhat reduce the computation cost, we are using surrogate-based optimization during which surrogates are fit to aerodynamic and structural responses.

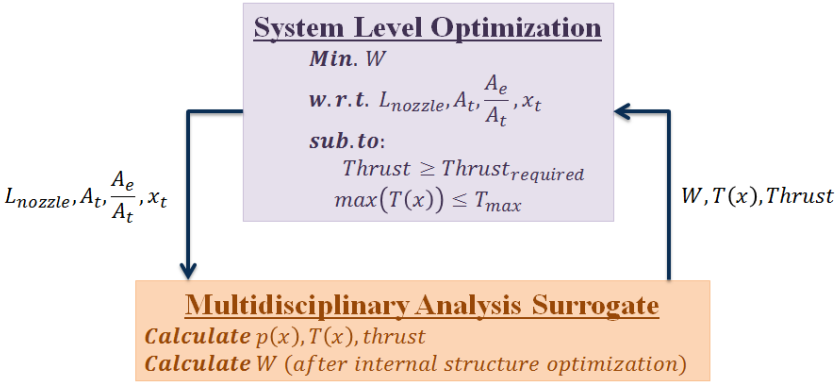

Figure 9: Monolithic optimization architecture with surrogates.

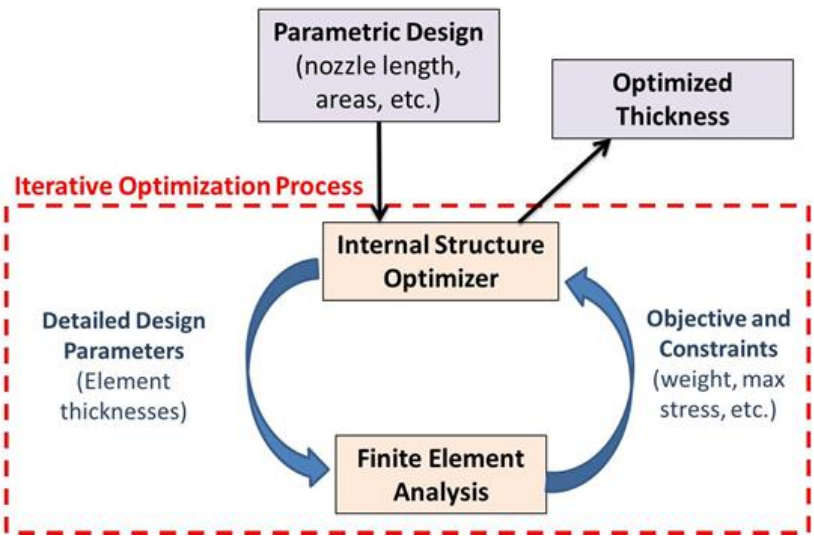

Figure 10: Schematic of the nested optimization process for structural sizing.

In the future, we will investigate alternate MDO architectures for efficiency improvements.

One architectural change that we are however implementing for cost reduction, is the use of a nested optimization approach. We know that the substructure members do not affect the aerodynamic analysis. Hence, these are local variables in structural analysis (the tie, nozzle and longeron thicknesses) that need not be included in the system level optimization. These values can be optimized separately in a substructure sizing process as shown in Figure 10. This process is motivated by work in multi-fidelity weight estimation techniques in a conceptual design environment [21] [20]. Basically, for a given set of shared variables (nozzle shape design variables), we can use FEA for the detailed internal structure design using optimization within the structural analysis only. This results in optimized thicknesses, while satisfying stress constraints and trying to minimize weight. The aero-thermal analysis computes the pressure and thermal loads, which are fed to the structural

analysis. The structural analysis uses these inputs to optimize the substructure and determines the weight, and temperatures in the structure (for fixed nozzle shape).

This architecture is implemented in the DAKOTA software suite. DAKOTA was originally intended to provide a flexible interface between simulation codes and iterative methods and strategies, however DAKOTA also supports multiple optimization methods and strategies, including multi-fidelity surrogate based optimization [19]. In terms of optimization, DAKOTA supports DOT and NPSOL methods for constrained optimization and OPT++ method for unconstrained. Among these, the user gets a choice of Broyden-Fletcher-Goldfarb-Shanno (BFGS), Fletcher-Reeves conjugate gradient method, modified method of feasible directions, sequential linear programming, and Sequential Quadratic Programming (SQP). DAKOTA is also capable of constructing surrogate models from aerodynamics and structures. In particular, it supports Kriging-based and polynomial surrogates, with several Design of Experiment (DOE) options; as well as trust region management methods [19]. In this work, we are using several of these capabilities for enabling the COMANDO vision.

D. Aerodynamic Optimization

In order to develop the optimization capability, we begin with a single disciplinary optimization – using Euler-based aerodynamic analysis. Note that since the Euler analysis is not affected by the length of the nozzle and location of throat, we have only two design variables in the optimization – areas of throat and exit. This allows us to quickly setup the optimization architecture and debug various pieces of the interface code. We first address the generation of surrogates for surrogate-based optimization (SBO).

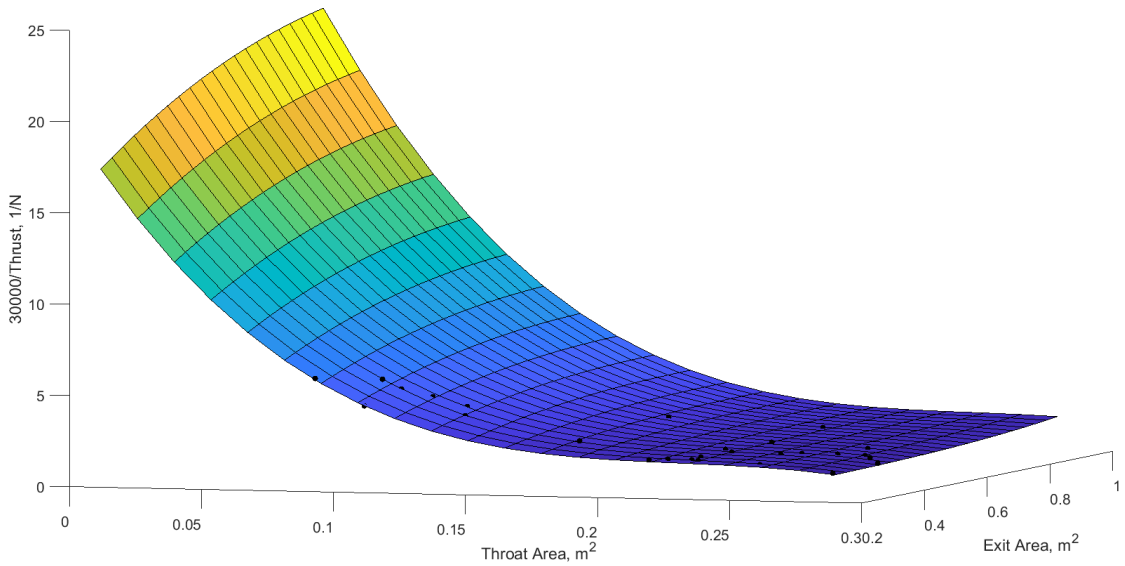

Figure 11: Example surrogate fit and data points (black dots) for the aerodynamic objective function.

For SBO, we experimented with several surrogate types (such as Kriging and polynomials) and decided to use cubic polynomials for this design study. Note that the choice depends on the data generated in the select design space, number of modes, etc. The surrogates are constructed using DAKOTA's in-built capabilities, which can also directly interface with the optimization. Figure 11 shows an example of the surrogate fit for the inverse thrust (the objective function for aerodynamics-only optimization) as a function of the two design variables of interest. The data points (shown as black dots) correspond to fully converged results. Filters were added to the batch mode aerodynamic simulation capability to automatically filter out the unconverged results. Some regions of the design space do not have supporting data, due to convergence issues (as can be expected for arbitrary nozzle shapes), but the overall trends from the surrogate are correct.

This surrogate is used for aerodynamic optimization for maximizing thrust. The design variables and their ranges are:

- Throat area, Athroat (0.001 – 0.279 m2)
- Exit area, Aexit (0.2919 – 1.0 m2)

Note that some of these ranges for the design variables are chosen to conform to the 9 knot parameterization we are using for the spline fit to the nozzle geometry. For the automated analysis to work, we implement a "catch" mechanism to ignore the cases that are unable to converge or cannot generate a good quality mesh. For such cases, in order to avoid pausing or stopping the optimization, we assign a large value for the inverse thrust (objective function). Also note that several robustness features have already been added to SU2 [32], to allow smooth convergence in most cases, as described in previous papers. Figure 12 shows the convergence history of the thrust during the optimization, and we will compare these results with direct aerodynamic optimization (no surrogates) next.

We try the case of direct analysis-based optimization next, to serve as a benchmark. In this case, DAKOTA directly calls the Euler analysis for optimization. The results of the optimization are shown in Figure 13. As we observe, the optimizer converges successfully and with fewer function evaluations than the SBO method. This might have to do with the starting point for the optimization, but it is not a cause of concern, since the evaluation of the polynomial fit is instantaneous. We further compare the results numerically between direct and surrogate-based optimization, in Table 2. We can see that the SBO process yields the same exact optimum as the direct optimization, and both lead to significantly better performance than the baseline. While, we cannot guarantee that SBO will capture the same optimum as direct optimization in each instance; we can at least claim both optimizations converge well. This system level optimization architecture is easily modified to use the multidisciplinary analysis architecture as well.

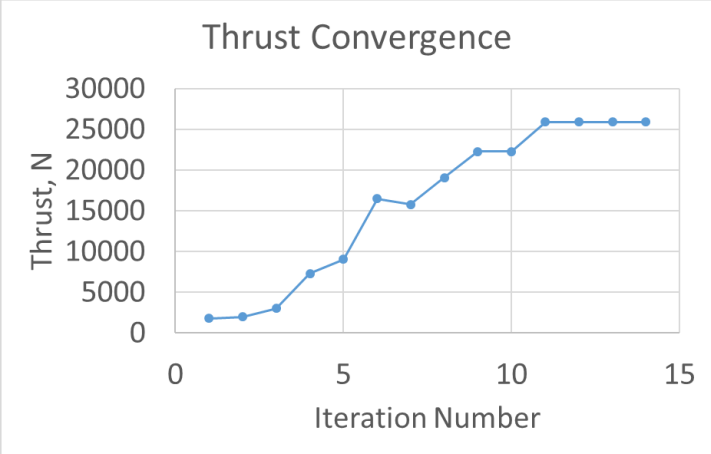

Figure 12: Convergence history of thrust, using SBO.

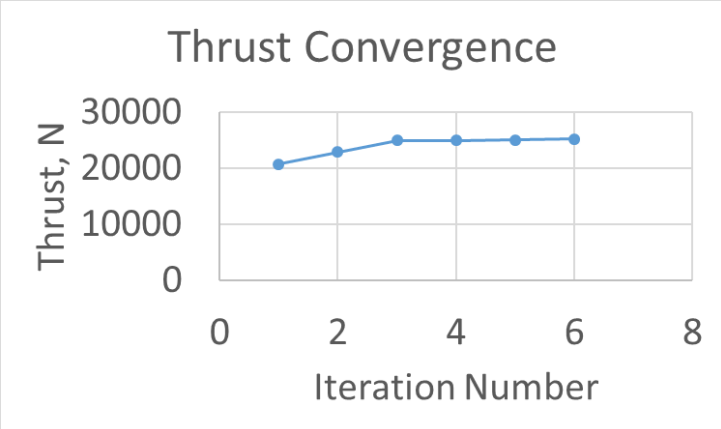

Figure 13: Convergence history of thrust, using direct optimization.

Table 2: Comparison of direct and surrogate based optimization with baseline values.

	Throat Area (m^2)	Exit Area (m^2)	Thrust (N)
Baseline Case	0.244	0.2919	20,914
Direct Analysis Optimization	0.279	0.2919	25,190
Surrogate Based Optimization	0.279	0.2919	25,190

E. Substructure Optimization

As mentioned before, we are using a nested optimization architecture for design that optimizes the substructure geometry within the structures discipline. This allows reducing the system level optimization cost. The substructure optimization problem is posed as:

$$Minimize: W_{substructure}$$
$$w.r.t.: t_{nozzle}, t_{tie}, t_{longeron}$$
$$subject\ to: max\big(\sigma(x,y,z)\big) \leq \sigma_{yield}$$

In order to enable this, we used the ANSYS built-in optimizer to optimize the thicknesses of substructure members (ties, longerons) and nozzle duct. This tends to be a more efficient option compared to coupling a generic optimizer to the FEA, since it makes use of structure-specific formulations for efficiency. Also, to enable the optimization, various parts of setting up the model in ANSYS, solution and post-processing, need to be automated. Specifically, we performed the following:

1) Developed mechanisms to accept the results from CFD analysis (pressures, temperatures and heat fluxes) as load-inputs for structural analysis
2) Developed scripts to conduct FEA in ANSYS (.inp files) automatically
3) Developed scripts to conduct optimization of the substructure in ANSYS Workbench (.wbjn files) automatically

4) Developed scripts in Python to compile appropriate .inp and .wbjn files based on user inputs

This process includes regeneration of substructure geometry for each iteration of the optimizer and transfer of aerodynamic loads as the structure mesh changes. In addition, we have developed a capability to be able to change the tie and longeron locations as well within the Workbench environment, but have not made it part of the optimization yet. Figure 14 shows an example solution for the optimization. As we can see, a feasible solution (maximum stress of 873 MPa, with yield stress at 990 MPa) is obtained, whereas the baseline solution was infeasible.

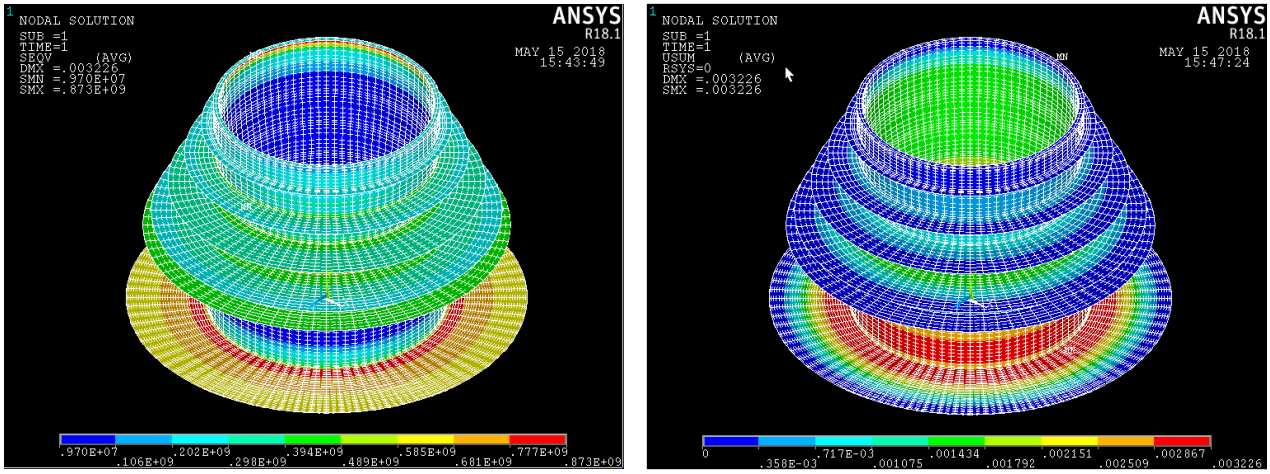

Figure 14: Sample optimization result from substructure optimization. The nodal Von Mises stress (left) and displacements (right) are shown. Feasible results are obtained through the optimization.

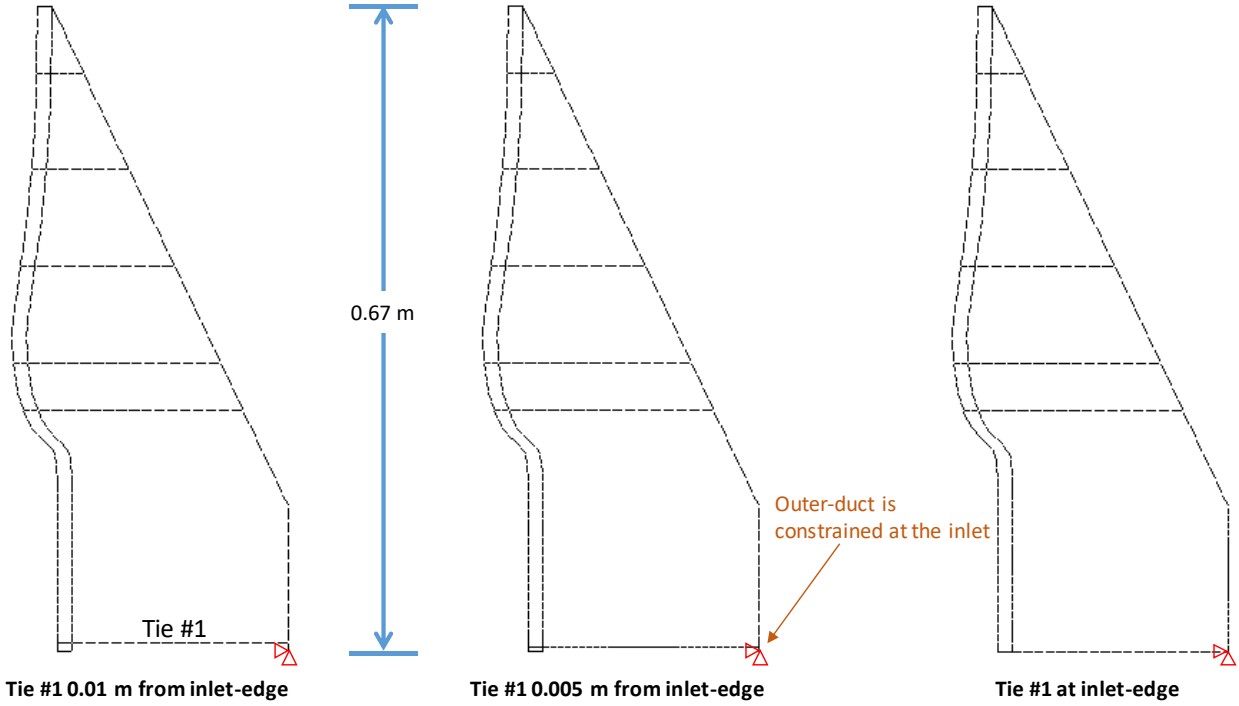

Figure 15: Substructure optimization with new locations for Tie #1, with Tie #2 position held constant.

Using the optimization scheme, we were able to achieve feasible results and reduction in weight of the nozzle. To investigate the impact of design parameters on the optimality, the number of design parameters (thicknesses of ties, longerons and liners) was steadily increased to eventually include all thicknesses as variables. That is, thicknesses of ties, longerons and liners vary independently of one another, leading to twelve variables. Implementing substructure optimization with this setup did not result in a feasible solution. Analysis of the results indicated that the location of ties can lead to stress concentrations, thereby violating the stress constraint criterion (maximum von Mises stress ≤ yield strength of material). To investigate this effect, location of the two ties closest to the nozzle inlet was varied—the second

tie from the inlet (Tie #2) was moved away from the throat of the nozzle and held constant, and the position of tie closest to the inlet (Tie #1) was varied to three positions (Figure 15). Substructure optimization was performed for these three configurations of the substructure and an optimal solution was found for each case (Table 1). As mentioned earlier, the position of ties within the substructure was not implemented as a design parameter within the automated optimization framework, and will be included in the future version of the COMANDO tool. The inclusion of buckling analysis within substructure optimization can constrain the solution from leading to very thin structures. However, this was not completed at the time of this paper due to the computational cost involved with undertaking buckling analysis.

Table 1: Results of substructure optimization for substructure configurations shown in Figure 15.

Case	Max. von Mises stress (GPa)	Total mass of structure (kg)
Tie #1 0.01 m from inlet-edge	0.85	163.82
Tie #1 0.005 m from inlet-edge	0.9899957	143.34
Tie #1 at inlet-edge	0.96	148.83

F. Aeroelastic Surrogate

With good confidence in our aerodynamic SBO capability, we decide to perform SBO for the aeroelastic design problem. First surrogates must be fitted to data from the MDA, which includes the substructure optimization. Also note that since structural analysis requires loads from aerodynamics, we need to perform structural analysis only on the points where CFD converged and gave reasonable results. Assuming that there may be cases where the structural analysis itself may not converge, the final set of data points from MDA would be a subset of points for which CFD converged.

In order to run the structural analysis in batch mode, we created Python scripts to extract the geometry and load data from the aerodynamic analysis and use that to run the structural analysis. Both the results are then parsed to create a common data file that can be used for aero-structural optimization. Note that we have selected a particular substructure geometry for this purpose (consisting of 6 ties and no longerons). Also, we consider a dual liner case here. With these assumptions, the entire process is automated to create the data file. Note that there are 10 responses in this case – mass is the objective function and there are 9 constraints (thrust, and stresses in ties, inner liner, and outer liner). Also, instead of the *conmin* optimizer which was being used earlier (for unconstrained optimization), we use DAKOTA's *optpp_fd_newton* method.

Unfortunately, the coupled optimization converges to unrealistic designs, which is likely due to inaccuracies in the surrogates. The surrogates for the mass and stress constraint in tie 1 (i.e. $max\big(\sigma(x,y,z)\big) - \sigma_{yield}$) are shown in Figure 16. Note that the black dots are the actual data points and the predictions are the surfaces themselves. We observe that the fit is predicting reasonably well in the vicinity of the data points, but outside of those regions, the extrapolation is somewhat arbitrary. This is to be expected, since we do not have data points in those regions. This is probably the contributing factor to the failure of the optimization. In order to rectify the issue, we will either need to refine our design space or obtain data in these regions. We are in the process of examining this issue and will provide results for the optimization in the future.

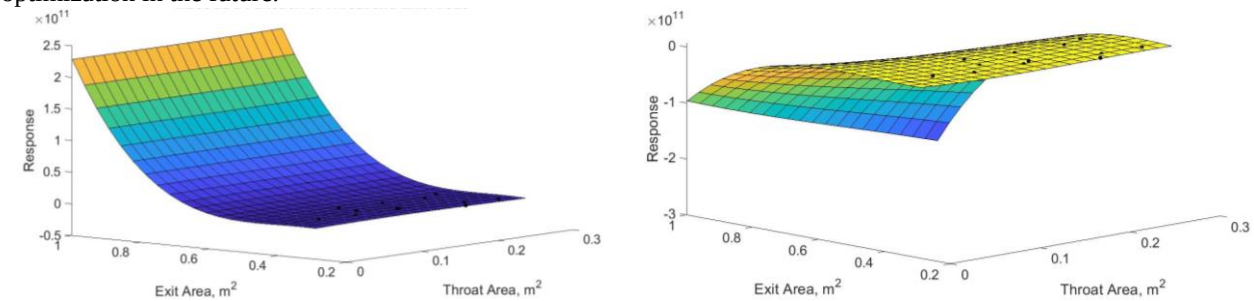

Figure 16: Surrogates for (a) mass, and (b) stress constraint in tie 1.

VII. COMANDO Toolset

Another goal of this research is to develop a toolset that can be used for design optimization of exhaust systems, which is easy to use and automates the most complex part of the capabilities. This toolset is currently focused on the modified NPARC nozzle discussed above, but will be made more generic in the future. Moreover, all the features and capabilities described in this paper are not yet part of the tool. Currently, the tool allows the user to perform standalone aerodynamic and structural analyses, substructure optimization, direct aerodynamic optimization and SBO for aerodynamics. The tool is currently a beta version, showcasing the main features to be made available in the final version and giving an example for some of them. The tool development was guided by two objectives:

1) Provide a User Interface (UI) for easy configuration and execution of features.
2) Provide an easy installation requiring minimal tool-specific installation support:
    a. Installation approach is agnostic to platform and Operating System (OS) version.
    b. Installable by end user with minimal knowledge about the installation process – step by step installation instructions are provided.
3) Provide minimal footprint on the host machine, after the installation.

Based on these criteria, we implemented a UI based on the Grails web application framework to interface and execute commands and render results. We also used a Docker approach for deploying and delivering the COMANDO software and the UI. Docker is a container approach for creating, deploying and running applications. We followed this containerization approach for the COMANDO software because it

- automates build process,
- can build-once, run-anywhere by containerizing the software along with the OS,
- follows the platform-as-service, software-as-service approach,
- reduces installation time: for e.g., COMANDO installation directly on host takes about 2 hours for installation (assuming we do not run into issues), but only 10-15 minutes using a Docker,
- improves scalability and can be installed multiple instances easily, and
- provides more confidence in the builds – we do not have to test the installation each time.

Since COMANDO has multiple sub-software components with many dependencies, we want to bundle and deploy it in isolation with any other software running on a host machine (except a Docker Host). As a result of these design choices, the COMANDO UI provides a centralized view to manage the configuration and execution of various features of the tool (providing input parameters, running and monitoring the simulations, and viewing and download the results). The UI can be run the same server as the tool and be extended to manage multiple COMANDO tool instances. Moreover, the tool can be accessed locally or remotely (within the organization's network or over the internet based on the security policies). The beta version of the tool was successfully deployed on the Navy's computer network.

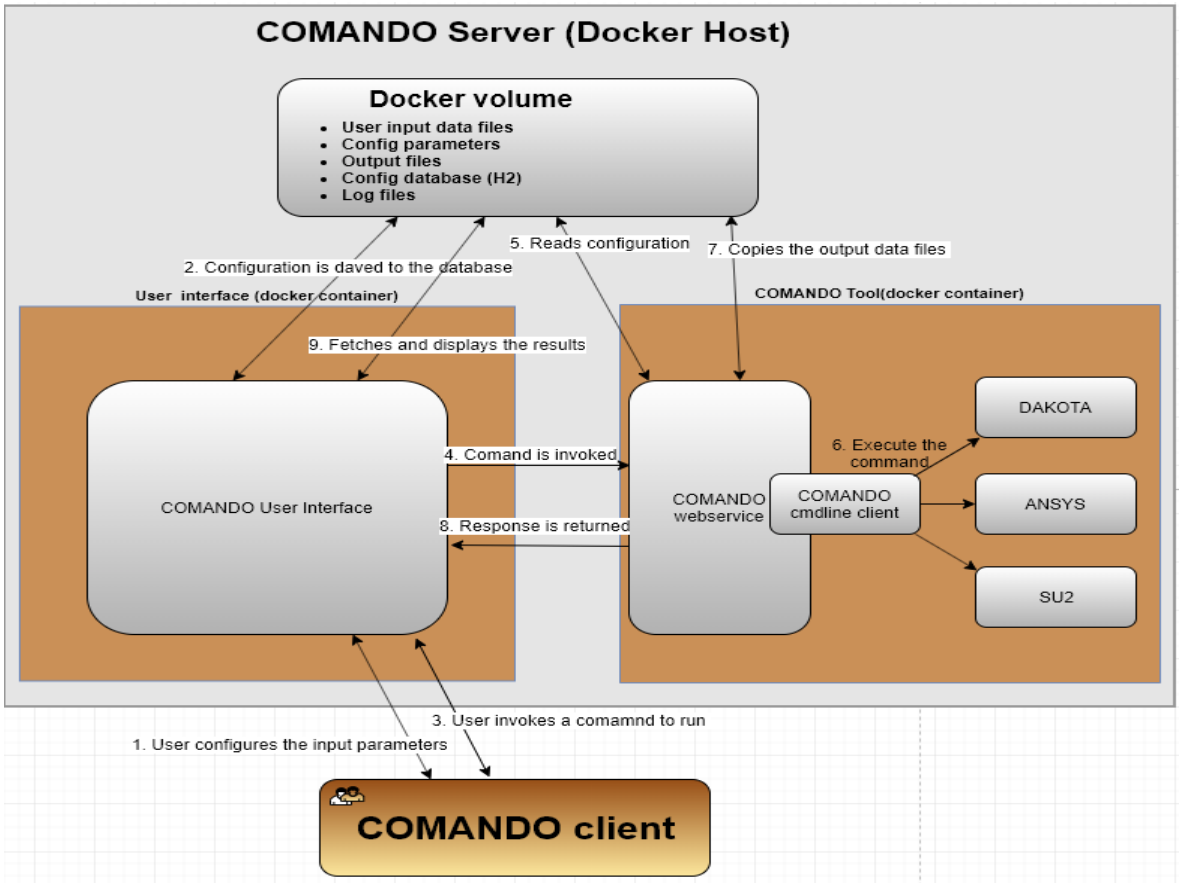

Figure 17: COMANDO tool deployment scheme and workflow.

We created two Docker containers one for the COMANDO software and the other for the UI. The orchestration of the components deployed is explained using the deployment diagram shown in Figure 17. The components include:

- COMANDO Docker container: The main software components (SU2, DAKOTA, and ANSYS), along with our Python scripts for interfacing and dependencies are deployed together into a single Docker container.
- GUI tool Docker container: This embeds a ZeroMQ client to send requests to the ZeroMQ server which then get executed on the COAMNDO software.
- Docker volume: By the nature of Docker, any data that gets created on a Docker container is temporary and gets deleted once the container is shutdown. In order for the data such as input configuration parameters, input and output data files to survive the Docker shutdowns, part of the storage on the host filesystem is used by creating and linking it to the Docker containers.

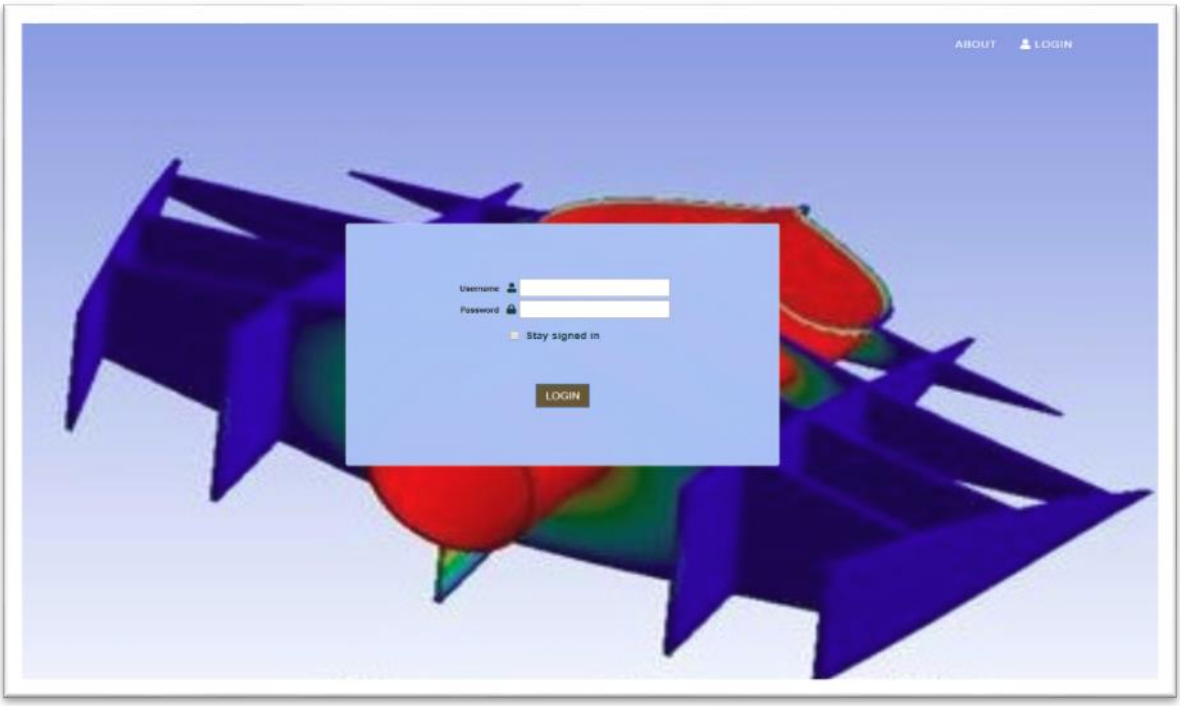

Figure 18: COMANDO tool login page snippet.

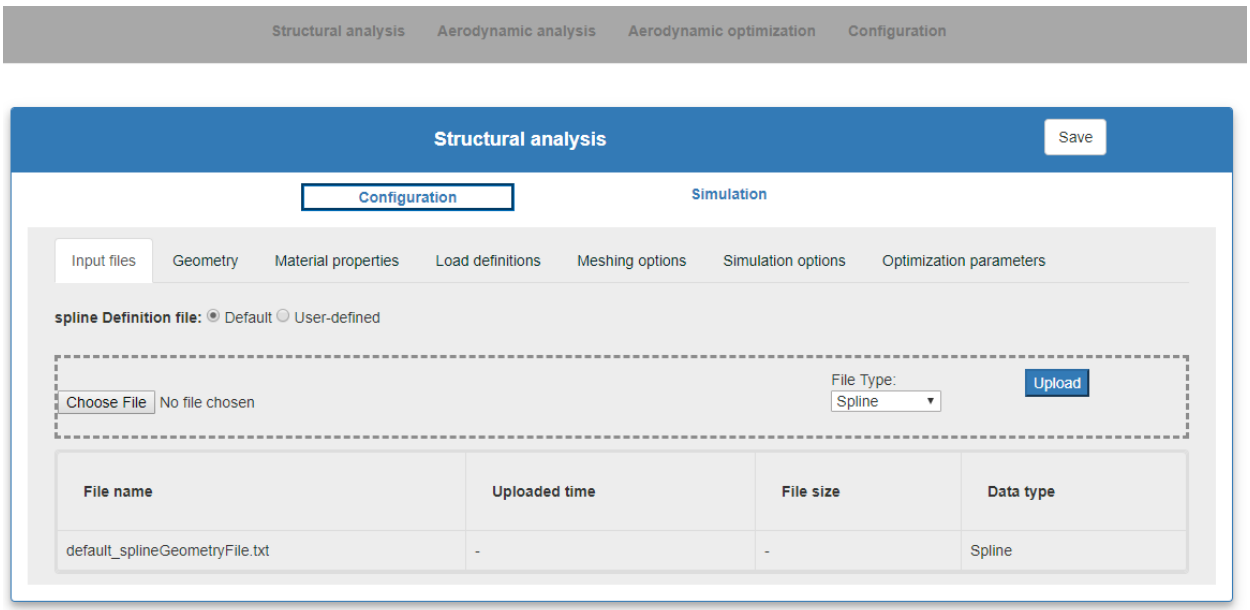

Figure 19: COMANDO dashboard and workflow options.

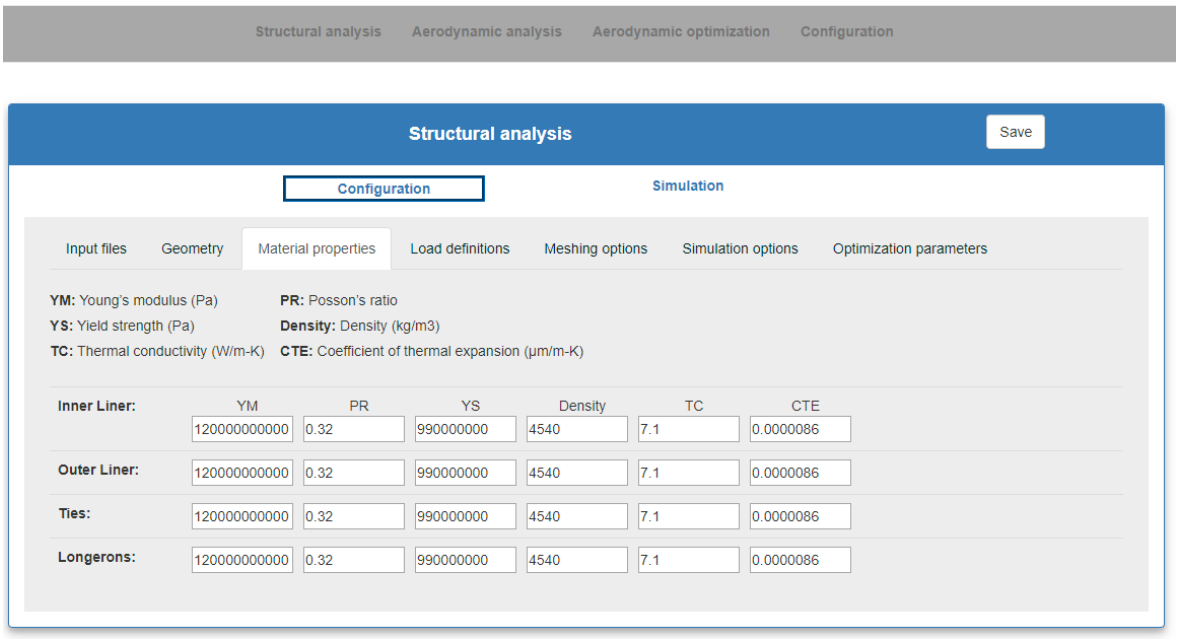

Figure 20: Structural analysis - Material properties.

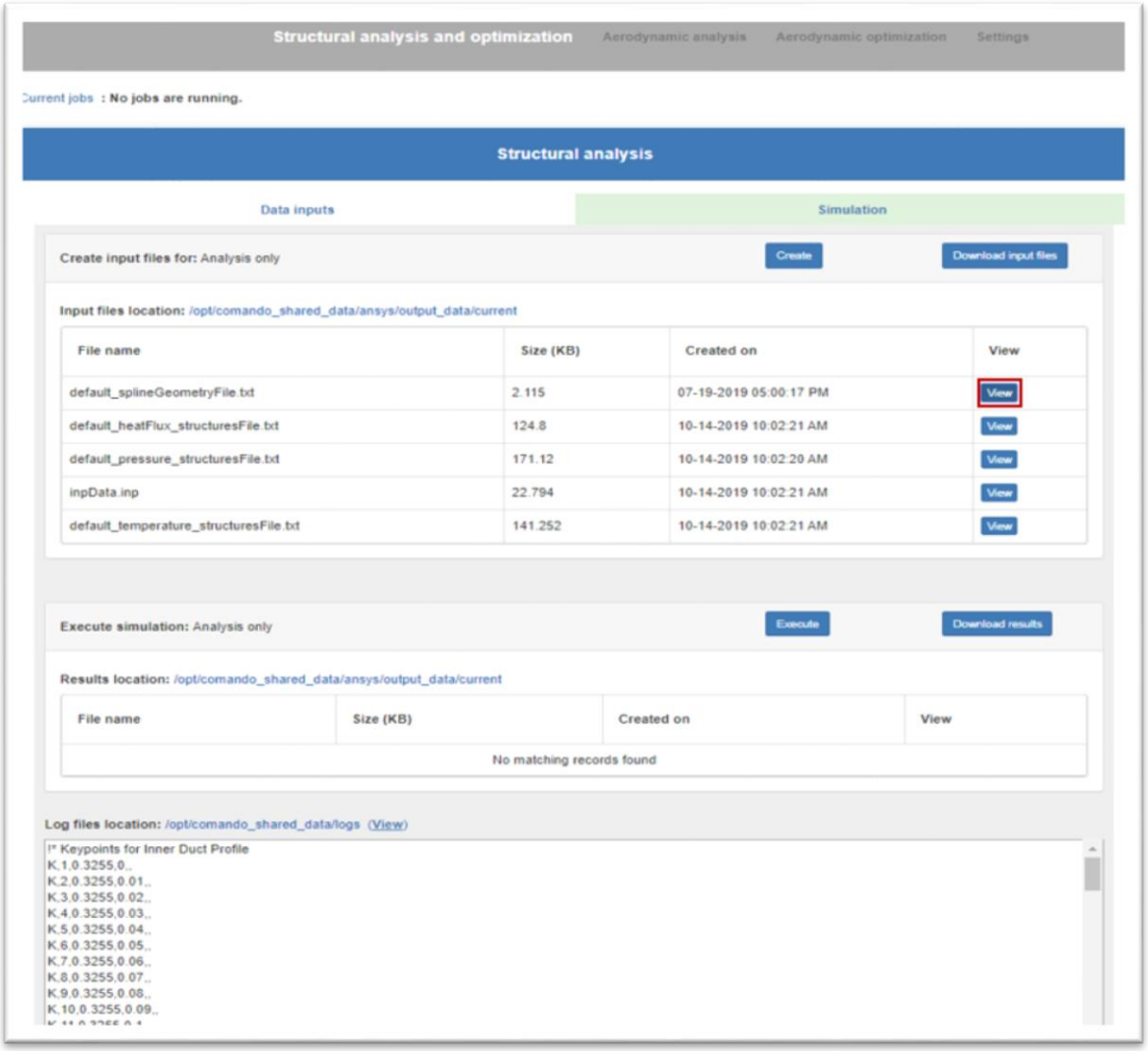

Figure 21: Creation of input file for ANSYS simulation (INP file).

To facilitate the interaction with COMANDO software and run the commands against it, a ZeroMQ server instance is integrated in a client-server mode listening for requests on a given port 5555. ZeroMQ is a light-weight high-performance asynchronous messaging library. To interpret and execute the client requests, a command execution client is implemented. This component based on the request type will execute a command against SU2 and ANSYS software similar to a command line client.

The UI is implemented using Grails 3 which is an open source web application framework built on top of Spring Boot and Apache Groovy programming language. Access to the tool is controlled by user authentication by userId and password as shown in Figure 18. Once logged in, a dashboard (see Figure 19) is displayed with a header containing links to three workflow paths: (1) Structural analysis (with substructure optimization), (2) Aerodynamic analysis, and (3) Aerodynamic optimization. Each workflow path has a "Configuration" section for capturing the user inputs and "Simulation" section for executing the commands. Default configuration values are provided for certain parameters, and users can overwrite them. As an example, the default configuration for structural analysis provided in a tabbed interface where each tab facilitates capturing of user input data of certain type - Figure 20 shows the screenshot for material properties. Once the configuration data is provided, user can execute the commands in the Simulation section. Figure 21 shows the results of INP file creation for structural analysis, and Figure 22 shows example results for ANSYS execution. Users can download the output data files using the "Download" button as well, if they want to analyze them later.

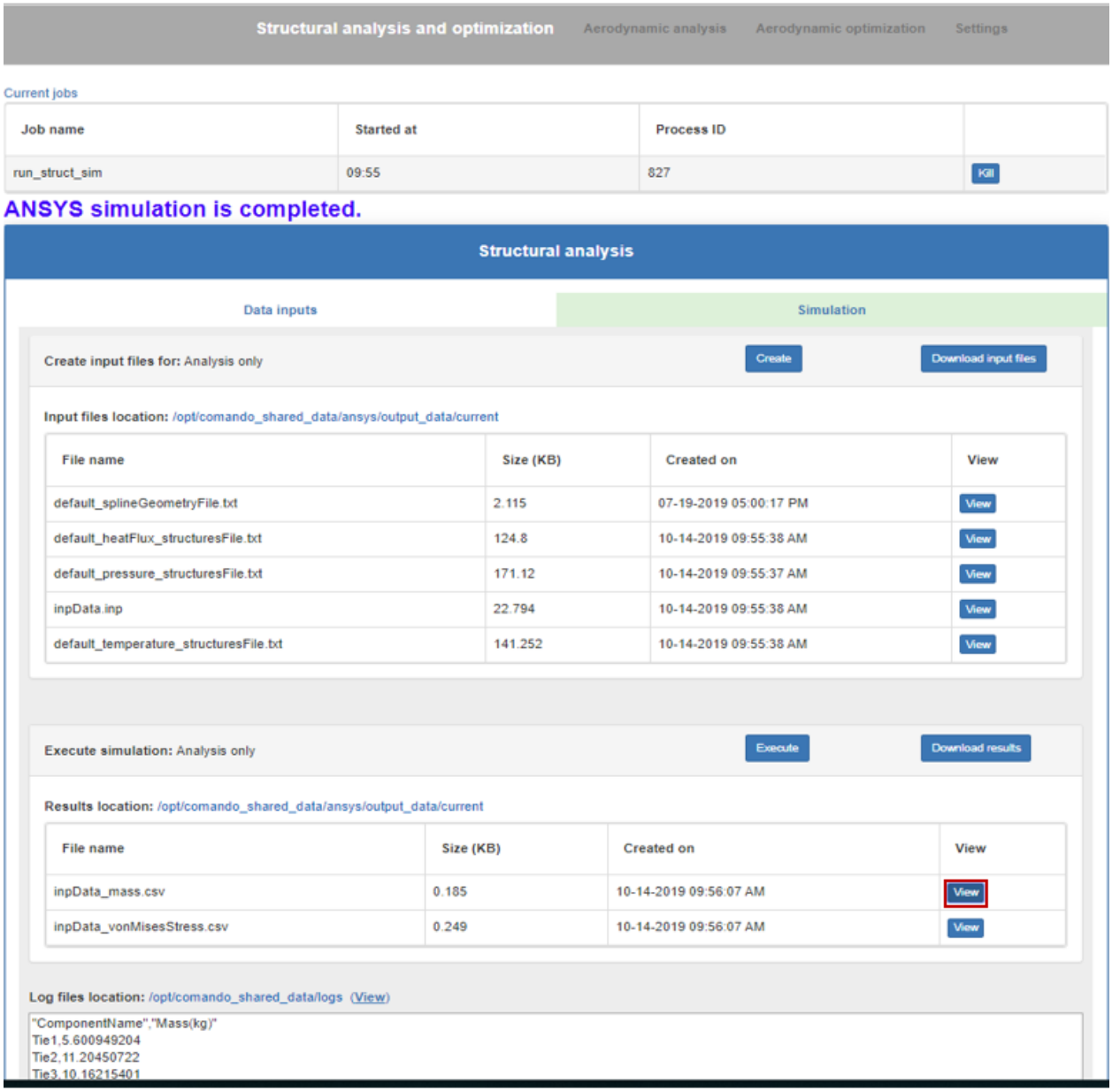

Figure 22: Visualization of ANSYS output results through UI.

The above screen captures show the UI layout and features for structural analysis. Similar features have been built-in for aerodynamic analysis (offering the option of Quasi-1D, Euler and RANS) and aerodynamic optimization (direct and SBO). This beta version of the tool provides an initial proof-of-concept for the envisioned toolset, and it is continuing to be developed for additional features, capabilities as well as application to user defined geometries.

VIII. Conclusion

This paper describes our ongoing efforts in developing a design optimization architecture for advanced jet engine exhaust systems. A crucial first step is the ability to analyze different configurations and capture the relevant physics. For this purpose, aerodynamic and structural analyses have been carefully developed and results examined. In particular, the structural analysis requires knowledge of the substructure as well – to sidestep this issue, we have developed a substructure sizing capability that can provide realistic estimates of the substructure configuration. The analyses are now being incorporated in an MDO architecture that supports both direct and surrogate-based optimization. A nested architecture is being developed to reduce the computational cost, wherein the substructure sizing is conducted within the structural analysis subspace. The optimization capability has been demonstrated for single discipline optimization and substructure optimization. Headway has been made with the development of surrogates for aerothermoelastic optimization, but some issues remain in the aeroelastic analysis. We have also been developing a user-friendly front end to the software to facilitate rapid design and analysis of nozzle configurations; and ease of installation on different platforms. Dockers are being used for this purpose, and we demonstrated a beta version of the tool that has been deployed at the customer site.

In the future, we will continue to add features and capabilities to the tool to enable user-driven surrogate generation, aero-structural design, and application to generic nozzle concepts. In parallel, our team has also been developing WMLES capabilities and analyzing inlets for engines. Eventually, these capabilities will also be integrated in the tool.

Acknowledgments

The research in this effort is being conducted under the U.S. Navy SBIR/STTR program. We thank NAVAIR for sponsoring this research. We also thank Navy personnel (Dr. Michael Lurie, Dr. John Spyropoulos, and Dr. Russell Powers) and Pratt and Whitney personnel (Mr. Rick Labelle, and Dr. Kerwin Low) for their extremely useful suggestions and continued support through technical discussions.

References

[1] M. Schwartz, K. Blakeley and R. O'Rourke, "Department of Defense Energy Initiatives: Background and Issues for Congress," Congressional Research Service, 2012.

[2] K. Osborn, "Lowering Prices on Biofuels Offers Navy Hope," Military.com, 2013. [Online]. Available: http://www.military.com/daily-news/2013/08/07/lowering-prices-on-biofuels-offers-navy-hope.html. [Accessed 2014].

[3] A. Andrews, "Department of Defense Fuel Spending Supply Acquisition and Policy," Congressional Research Service, 2009.

[4] NASA, "Subsonic Fixed Wing - Research Overview," National Aeronautics and Space Administration, 2012. [Online]. Available: http://www.aeronautics.nasa.gov/fap/sfw_research_overview_feature.html. [Accessed 2012].

[5] L. S. Hultgren, "CORE NOISE: Implications of Emerging N+3 Designs and Acoustic Technology Needs," NASA, Cleveland, Ohio, 2011.

[6] S. Martens, J. T. Spyropoulos and Z. Nagel, "The Effect of Chevrons on Crackle: Engine and Scale Model Results," vol. 1, 2011.

[7] J. W. Nichols, F. E. Ham, S. K. Lele, Y. Khalighi and J. Spyropoulos, "High-Fidelity LES of Asymmetric Supersonic Jets," 2011.

[8] R. J. Shyne, "A Survey of Challenges in Aerodynamic Exhaust Nozzle Technology for Aerospace Propulsion Applications," NASA, 2002.

[9] S. Martens and J. T. Spyropoulos, "Practical Jet Noise Reduction for Tactical Aircraft," vol. 1, 2010.

[10] W. J. Voorhees, "Versatile Affordable Advance Turbine Engine (VAATE)," NAVAIR, 2007.

[11] F. R. Menter, "Two-Equation Eddy-Viscosity Turbulence Models for Engineering Applications," vol. 32, no. 8, 1994.

[12] H. Doi and J. J. Alonso, "Fluid/Structural Coupled Aeroelastic Computations for Transonic Flows in Turbomachinery," 2002.

[13] E. A. Thornton, Thermal Structures for Aerospace Applications, Reston, VA: American Institute of Aeronautics and Astronautics, Inc., 1996.

[14] J. D. Deaton and R. V. Grandhi, "Stiffening of Restrained Thermal Structures via Topology Optimization," vol. 48, pp. 731-745, 2013.

[15] J. J. Korte, A. O. Salas, H. J. Dunn, N. M. Alexandrov, W. W. Follet, G. E. Orient and A. H. Hadid, "Multidisciplinary Approach to Aerospike Nozzle Design," NASA, 1997.

[16] S. Kodiyalam and J. Sobieszczanski-Sobieski, "Multidisciplinary Design Optimization - Some Formal Methods, Framework, Requirements and Applications to Vehicle Design," vol. 25, no. 1/2, pp. 3-22, 2001.

[17] F. Palacios, K. Duraisamy, A. Aranake, S. R. Copeland, T. D. Economon, A. K. Lonkar, T. W. Lukaczyk, K. R. Naik, S. Padron and J. J. Alonso, "Stanford University Unstructured (SU2): Analysis and Design Technology for Turbulent Flows," 2014.

[18] M. S. Eldred and D. M. Dunlavy, "Formulations for Surrogate-Based Optimization with Data-Fit, Multifidelity and Reduced-Order Models," 2006.

[19] M. S. Eldred, A. A. Giunta and S. S. Collis, "Second Order Corrections for Surrogate-Based Optimization with Model Hierarchies," 2004.

[20] N. Nigam, S. Ayyalasomayajula, X. Qi, P. C. Chen, J. J. Alonso and A. Variyar, "High-Fidelity Weight Estimation for Aircraft Conceptual Design Optimization," 2015.

[21] F. H. Gern, "Conceptual Design and Structural Analysis of an Open Rotor Hybrid Wing Body Aircraft," 2013.

[22] J. D. Deaton, "Design of Thermal Structures Using Topology Optimization," Ph.D. Thesis, Wright State University, 2014.

[23] Sandia National Laboratories, "DAKOTA, A Multilevel Parallel Object-Oriented Framework for Design Optimization, Parameter Estimation, Sensitivity Analysis, and Uncertainty Quantification. Users's Manual Version 5.4," Sandia National Laboratories, Albuquerque, New Mexico 87185, 2014.

[24] J. W. Slater, "NPARC Alliance Validation Archive," 2008. [Online]. Available: http://www.grc.nasa.gov/WWW/wind/valid/axinoz/axinoz.html. [Accessed 2016].

[25] N. Nigam, S. Ayyalasomayajula, Y. Tang, P. Urbanczyk and J. J. Alonso, "Design Optimization of Advanced Exhaust Systems," *AIAA Multidisciplinary Design Optimization Conference*, 2017.

[26] P. Urbanczyk, J. J. Alonso, N. Nigam, X. Qi, A. Tyagi and P. Chen, "Coupled Multiphysics Analysis for Design of Advanced Exhaust Systems," 2017.

[27] S. R. Wellborn, B. A. Reichert and T. H. Okiishi, "An Experimental Investigation of the Flow in a Diffusing S-Duct," NASA, 1992.

[28] A. Jameson, W. Schmidt and E. Turkel, "Numerical solution of the Euler equations by finite volume methods using Runge Kutta time stepping schemes," in *14th Fluid and Plasma Dynamics Conference*, Palo Alto, 1981.

[29] C. Geuzaine and J.-F. Remacle, "Gmsh: A 3-D finite element mesh generator with build-in pre- and post-processing facilities," *International Journal for Numerical Methods in Engineering*, vol. 79, no. 11, pp. 1309-1331, 2009.

[30] A. Loseille and V. Menier, "Serial and Parallel Mesh Modifiation Through a Unique Cavity-Based Primitive," in *Proceedings of the 22nd Internal Meshing Roundtable*, Orlando, 2014.

[31] F. Alauzet and D. Marcum, "A Closed Advancing-Layer Method with Changing Topology Mesh Movement for Viscous Mesh Generation," in *Proceedings of the 22nd International Meshing Roundtable*, Orlando, 2014.

[32] R. Fenrich and J. J. Alonso, "Reliable Multidisciplinary Design of a Supersonic Nozzle Using Multifidelity Surrogates," *18th AIAA/ISSMO Multidisciplinary Analysis and Optimization Conference*, 2017.

[33] N. Nigam and I. Kroo, "Control and Design of Multiple Unmanned Air Vehicles for a Persistent Surveillance Task," 2008.

[34] N. Nigam, A. Tyagi, P. Chen, J. J. Alonso, F. Palacios, M. Ol and J. Byrnes, "Multifidelity Multidisciplinary Propeller and Rotor Analysis and Design," 2015.